Research Article

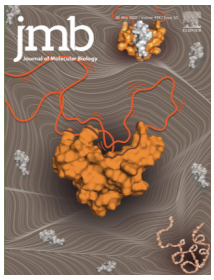

Topology of the SecA ATPase Bound to Large Unilamellar Vesicles

Guillaume Roussel [1] **Eric Lindner and Stephen H. White** [*]

Department of Physiology and Biophysics, *University of California, Irvine, Irvine, CA 92697-4560, United States* [1]

Correspondence to Stephen H. White: *stephen.white@uci.edu (S.H. White)*
https://doi.org/10.1016/j.jmb.2022.167607
Edited by Lutz Schmitt

Abstract

The soluble cytoplasmic ATPase motor protein SecA powers protein transport across the *Escherichia coli* inner membrane via the SecYEG translocon. Although dimeric in solution, SecA associates monomerically with SecYEG during secretion according to several crystallographic and cryo-EM structural studies. The steps SecA follows from its dimeric cytoplasmic state to its active SecYEG monomeric state are largely unknown. We have previously shown that dimeric SecA in solution dissociates into monomers upon electrostatic binding to negatively charged lipid vesicles formed from *E. coli* lipids. Here we address the question of the disposition of SecA on the membrane prior to binding to membrane embedded SecYEG. We mutated to cysteine, one at a time, 25 surface-exposed residues of a Cys-free SecA. To each of these we covalently linked the polarity-sensitive fluorophore NBD whose intensity and fluorescence wavelength-shift change upon vesicle binding report on the the local membrane polarity. We established from these measurements the disposition of SecA bound to the membrane in the absence of SecYEG. Our results confirmed that SecA is anchored in the membrane interface primarily by the positive charges of the N terminus domain. But we found that a region of the nucleotide binding domain II is also important for binding. Both domains are rich in positively charged residues, consistent with electrostatic interactions playing the major role in membrane binding. Selective replacement of positively charged residues in these domains with alanine resulted in weaker binding to the membrane, which allowed us to quantitate the relative importance of the domains in stabilizing SecA on membranes. Fluorescence quenchers inside the vesicles had little effect on NBD fluorescence, indicating that SecA does not penetrate significantly across the membrane. Overall, the topology of SecA on the membrane is consistent with the conformation of SecA observed in crystallographic and cryo-EM structures of SecA-SecYEG complexes, suggesting that SecA can switch between the membrane-associated and the translocon-associated states without significant changes in conformation.

Introduction

A key step in the biogenesis of secreted proteins is their translocation across the lipid bilayer of the plasma membrane. In *Escherichia coli*, this essential process is carried out by the general secretory (Sec) system that drives the secretion of proteins across the inner membrane into the periplasm. This conserved system consists of two key components, the hetero-trimeric transmembrane SecYEG complex that provides a pathway across the lipid bilayer and the soluble SecA ATPase motor protein that maintains secreted proteins in a translocation-competent

state.[1] The SecA-SecYEG complex[2] delivers secreted proteins into the periplasmic space by hydrolyzing ATP.[3]

The exact targeting mechanism of SecA to the cell membrane and the dynamics of its interactions with the SecYEG channel are poorly understood. *In vivo*, SecA appears to be distributed equally between a soluble dimeric state in the cytoplasm and a monomeric membrane-bound state in which negatively charged lipids are required for efficient protein translocation.[4,5] A fraction of the membrane-associated SecA-SecYEG population is thought to be integral *in vivo*, because it cannot be removed by treatments used to define proteins as peripheral.[6,7] Even in the absence of SecYEG, SecA binds to liposomes containing anionic lipids[8–11] mainly through electrostatic and hydrophobic interactions of the N- and C-terminal domains.[12] At the N terminus, which carries a net positive charge, deletion of the first 20 amino-acids results in loss of SecA activity.[5,13] When partitioned into liposomes formed from *E. coli* lipids, the N terminus forms an amphipathic helix that lies at the interface between the polar headgroups and the hydrophobic interior.[11,14] The last 30 residues of the C-terminal domain also interact with the membrane.[15] A bioinformatics study identified eight additional regions in the SecA sequence as possible lipid-binding sites.[16]

Knowing the exact disposition of SecA on membranes is important, because SecA apparently gains access to the SecYEG complex via a lipid-bound intermediate state that induces a change in conformation to prime SecA for high affinity binding to SecYEG.[5] A recent mechanistic study has suggested a kinetic pathway between cytosolic SecA and SecA-SecYEG complex via a membrane-associated state. In the resulting model, SecA first senses the membrane via its N terminus, forming a first intermediate that then binds tightly to the lipid membrane to form a long-lived (~10 secs) complex.[17] The model suggests that a membrane-associated intermediate of SecA plays a crucial role during translocation. However, there is little topological information about the structure of membrane bound SecA, which is critical for understanding the disposition of SecA on the membrane during the proposed first step of protein translocation.

We examine here the topology of SecA bound to large unilamellar vesicles (LUV) made from *E. coli* lipids using methods previously described.[10,11,18] Of particular importance in the present study is the observation that SecA dimers in solution dissociate into monomers upon partitioning into lipid bilayers.[11] We created a collection of 25 surface-exposed mono-cysteine mutants (Figure 1). We covalently linked to each cysteine, one at a time, the polarity-sensitive fluorophore 7-nitrobenz-2-oxa-1,3-diazol-4-yl (NBD). From the fluorescence intensity increases and wavelength shifts upon binding to LUV, the local polarity of each labeled residue was determined. We found that SecA is apparently anchored primarily in the membrane interface by the first 20 residues of the N terminus domain, a limited region of the nucleotide binding domain II, and the extreme C terminus of the protein. All three lipid-binding domains are rich in positively charged residues, consistent with electrostatic interactions playing a key role in membrane binding. Mutation of groups of positively charged residues to alanine resulted in weaker membrane binding and provided information on the relative importance of the domains in membrane partitioning. As expected, the N terminus is primarily responsible for initial membrane binding, while the other two domains seem more involved with the stabilization of the membrane-bound conformation. Overall, the conformation of SecA on the membrane appears similar to the conformation seen in crystallographic and cryo-EM structures of SecA-SecYEG complexes. This similarity suggests that SecA can move from the bilayer-bound state to the SecYEG bound state without major conformational changes.

Results

Membrane-bound topology of SecA

To determine the topology of monomeric SecA bound to lipid bilayers, we used a spectroscopic approach in which the environment-sensitive probe 7-nitrobenz-2-oxa-1,3-diazol-4-yl (NBD)[19] was covalently linked to cysteine residues of SecA engineered into the protein.[20] NBD fluorescence is sensitive to the polarity of the environment with an emission blue shift and fluorescence intensity (F) increase upon transfer from an aqueous to a less polar environment.[21,22] The local membrane environment of a labeled residue can thus be determined by comparing NBD-fluorescence measured in the absence (F_0) or presence (F) of lipid vesicles.[20,23,24] This specific behavior is widely used in monitoring the orientation and conformation dynamics of membrane proteins.[24–29] Here, we used F/F_0 as the measure of the extent of the interaction. To simplify analysis, fluorescence intensities were normalized so that the fluorescence intensity at 540 nm in the absence of vesicles was $F_0 = 1$.

As a proof of concept, we started with an N terminus G11C-SecA mutant,[30] which had been shown previously to penetrate the membrane interface at the headgroup/hydrophobic boundary.[14] We measured NBD-G11C-SecA fluorescence (F_0) in solution (Figure 2(A), black line) and 30 minutes after the addition of LUVs made from *E. coli* lipids (F, red line).[10] The fluorescence blue shift and intensity increase indicated that the Cys-NBD probe was located in the membrane region. Titration with LUV revealed (Figure 2(B)) a mole-fraction partition coefficient (K_x) of $213 \pm 14 \times 10^3$, corresponding to a free energy of transfer of SecA from water to bilayer (ΔG_{wb}) of -7.1 ± 0.1 kcal mol^{-1}. These val-

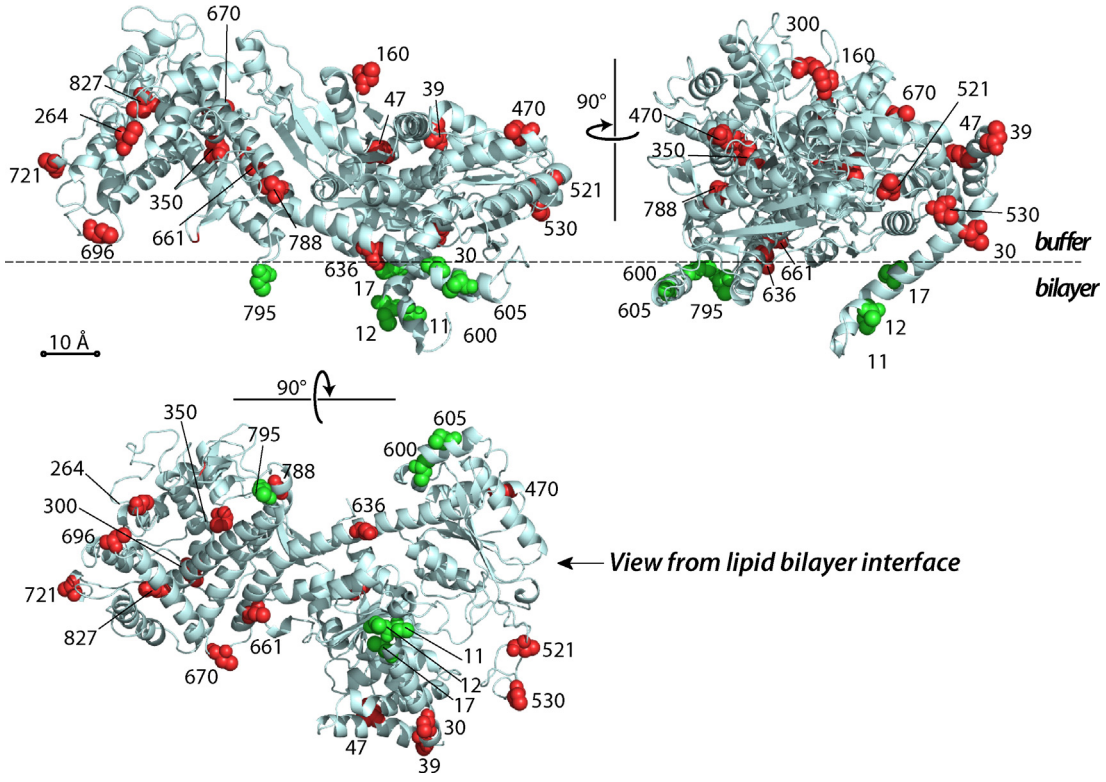

Figure 1. Topology of SecA bound to large unilamellar vesicles (LUV) formed from *E. coli* lipids. Single-Cys mutants of SecA labeled with the polarity-sensitive fluorophore 7-nitrobenz-2-oxa-1,3-diazol-4-yl (NBD)[19] were used to determine the topology of monomeric SecA on LUV. (Although SecA is dimeric in solution, the dimers dissociate into monomers upon partitioning into the LUV.[11] Starting with a Cys-free SecA mutant, each of the 25 residues shown were mutated one at a time to Cys. NBD was covalently linked to each Cys residue. From the NBD fluorescence increases and wavelength blue-shifts upon binding to the LUV, the local polarity of each NDB label was determined. The structure of *E. coli* SecA was modeled after the *B. subtilis* structure determined by Hunt et al.,[48] PDB:1M6N. The dashed horizontal line indicates the approximate location of the membrane-water interface. Residues colored green are those determined to be in close proximity to the membrane based upon large increases in fluorescence while those colored red show no significant fluorescence changes. See Figure 2.

ues matched our previous results obtained with unlabeled SecA,[10] indicating that the NBD probe had little effect on SecA partitioning into LUVs.

We therefore mutated, one at a time, the remaining 24 residues in a Cys-free SecA[30] (Table S1), covalently linked the NBD probe, and determined the local polarity of each probe using the change in NBD-fluorescence intensity (F/F_0) upon LUV binding, summarized in Figure 2(C). Each of the Cys mutants were able to complement $secA^-$ cells (Figure S1). The fluorescence data revealed that some labeled mutants were little affected by the presence of LUVs while others showed a major increases. The probes most affected by binding were those associated with the N terminus of the protein, as expected, but also those in the nucleotide binding domain 2 (NBD-2), the two-helix finger (2HF), and the C-tail of the protein. By coloring on the crystal structure of *E. coli* SecA the amino acid residues that exhibit strong NBD fluorescence increases in green and those largely unaffected in red, we determined the topology of the membrane-bound state (Figure 1).

SecA does not apparently cross the bilayer

When bound to *E. coli* membranes, it has been proposed that SecA may integrate *in vivo* into the membrane by itself, forming a stable transmembrane protein[7,31] despite the fact that SecA lacks hydrophobic segments sufficiently long to span the membrane.[32] To determine if any of the labeled residues on SecA cross the LUV bilayer, we used NBD fluorescence in combination with the Uniblue (UB) quencher.[27] If a SecA residue penetrates across the membrane, then NBD fluorescence exposed to the interior of vesicles should be quenched by UB trapped within the vesicles. As a positive control, we started with the NBD-S39C-SecA mutant with its unique cysteine pointing toward the buffer as proposed in our membrane-associated topology (Figure 1, Figure 2(C)). Figure 3 (panel C39) shows that addition of increasing concentrations of the UB to NBD-S39C-SecA in solution (black line) caused a dramatic decrease in fluorescence of about 50%, confirming the quenching effect of UB dye on the NBD fluores-

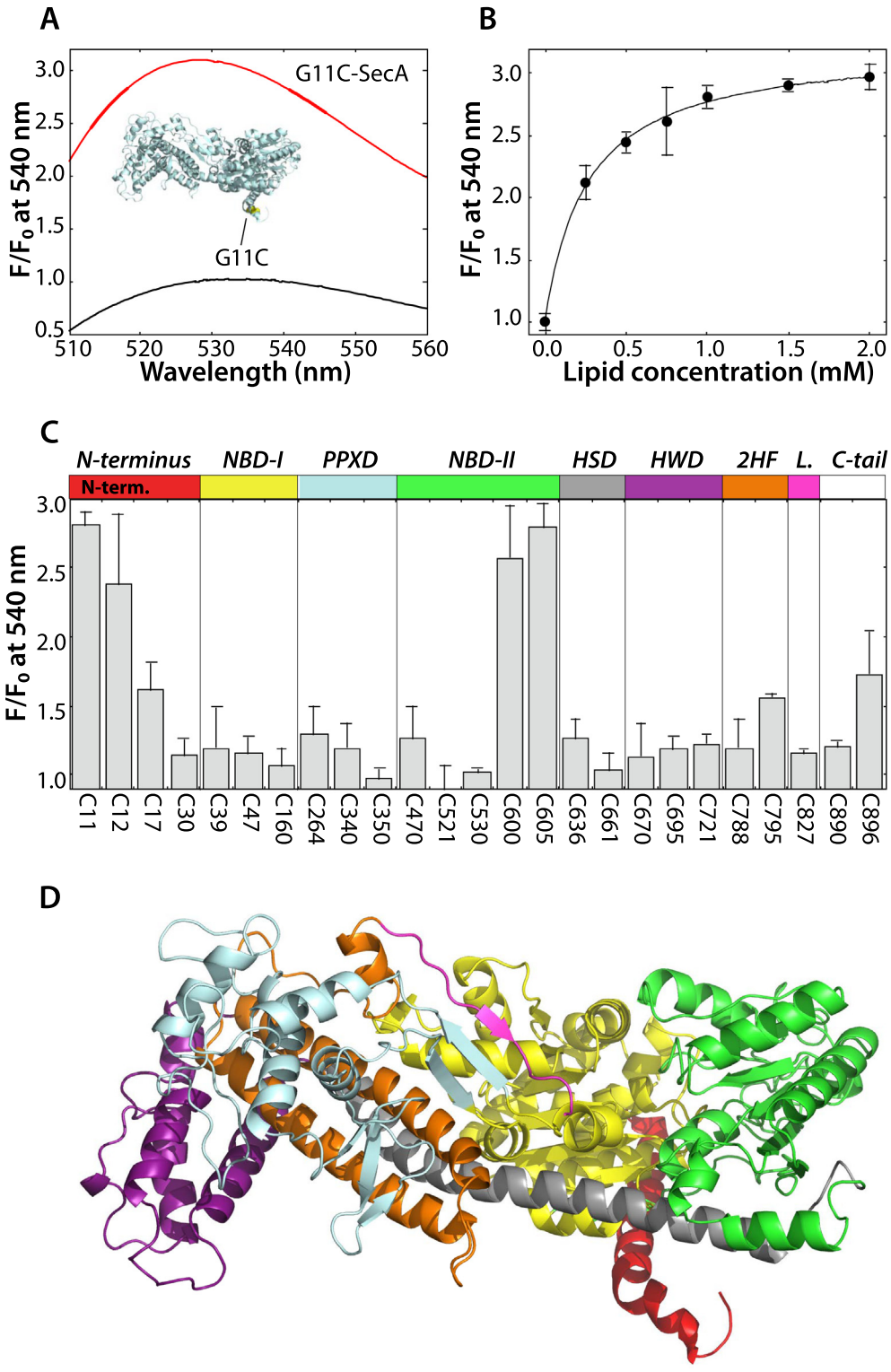
A
G11C-SecA
G11C
F/F0 at 540 nm
Wavelength (nm)
B
F/F0 at 540 nm
Lipid concentration (mM)
C
N-terminus
NBD-I
PPXD
NBD-II
HSD
HWD
2HF
L.
C-tail
N-term.
F/F0 at 540 nm
C11
C12
C17
C30
C39
C47
C160
C264
C340
C350
C470
C521
C530
C600
C605
C636
C661
C670
C695
C721
C788
C795
C827
C890
C896
D

cence. When UB was added in solution after partitioning of NBD-S39C-SecA to LUVs, a similar behavior was observed (red line), confirming exposure of the NBD-probe to the solvent even in the presence of the membrane. When NBD-S39C-SecA was mixed with LUVs containing the UB quencher inside, the NBD-fluorescence was not affected (blue line), meaning that the UB quencher remained in the lumen without access to the NBD probe. Similar trends were observed with other cysteine residues exposed to the solvent in our membrane-associated topology (Figure 3, left panel).

To see if any of the labeled parts of SecA cross the membrane, we started with NBD-G11C-SecA that interacts strongly with the bilayer. As shown in Figure 3, while the addition of UB probe resulted in a major decrease in NBD fluorescence in solution (black line), only a minor decrease in NBD fluorescence was observed when the quencher was added in solution after partitioning of SecA to LUV (red line), demonstrating that this cysteine residue is embedded in the membrane interface and therefore only weakly accessible to the quencher. When the UB probe was located inside the LUVs, no change in NBD fluorescence was observed (blue line), demonstrating that the cysteine did not cross the membrane. Using all the mono-cysteine SecA mutants that interact strongly with the bilayer (C12, C600, C605, C795, and C896, Figure 3, middle panels), we found that none of the five other NBD probes were significantly quenched by the UB probe inside the LUVs. There were variable responses to quencher outside the vesicles (red lines) that resulted from diffusion of the quencher into the membrane interface region. The variations hint at the likelihood that access depends upon the depth of burial of the probe in the membrane interface, which is about 15 Å thick.[33] Most important is that the NBD probes interacting with the lipid bilayer are not accessible from inside the LUV (blue lines).

Finally, we applied the same strategy to mono-cysteine mutants that are close to, but not embedded in the bilayer interface, according to our proposed topology (C530, C695, and C788) to see if they crossed the membrane (Figure 3, right panels). We observed, as expected, that those residues are variably exposed to the external solution but not the internal solution. Collectively, the above results demonstrate that, under our conditions, SecA is strictly surface bound without any indication of penetration of labeled residues across the membrane.

SecA has three lipid-binding domains

Figure 2(C) summarizes the regions of SecA that interact strongly with the negatively charged LUV interface. In *E. coli*, the essential first 24 residues of the N terminus contain an excess of 7 positively charged residues, consistent with the proposed membrane location (Figure 4(A)). It constitutes the first lipid-binding domain of SecA, as previously described.[5,14,17] Three of our NBD-labeled mutants (C11, C12, and C17) located in the N-terminal region showed a large increase in NBD fluorescence (Figure 2(C)), confirming that these residues are deep in the membrane interface.

A second lipid-binding domain was identified around the positions 600 and 605. The corresponding Cys-NBD mutants displayed a significant change in NBD fluorescence upon partitioning into LUVs. This region, named the Joint Domain (residues 591–621 in *ec*SecA),[34] is formed by an alpha-helix located between the Nucleotide Binding Domain II (NBD-II) and the first half of the Helix Scaffold Domain (HSD, see Figure 2

Figure 2. Increases in NBD fluorescence blue-shifts and amplitudes indicate the local environment of each NBD label. For each label, the fluorescence of SecA (1 μM) was recorded between 510 and 560 nm using an excitation wavelength at 470 nm in the absence (F_0) or presence (F) of large unilamellar vesicles (LUVs, 2 mM) formed from *E. coli* lipids. To simplify analysis, fluorescence intensities were normalized so that the maximum value of fluorescence in the absence of vesicles was $F_0 = 1$. **(A)** The fluorescence of the G11C NBD label in the absence (black line) and presence of LUVs (red line). The blue-shift and intensity increase of the fluorescence indicates that G11 near the N terminus of SecA is in the bilayer. See supplementary Figure S1 for fluorescence spectra for each labeled position. **(B)** Relative NBD fluorescence-intensity changes (F/F_0 at 540 nm) accompanying the titration of aqueous solutions of the NBD-labeled G11C SecA with LUVs. The black curve is a non-linear least-squares fit to the data (see Methods) from which the mole-fraction partition coefficient K_x was derived. In this case, $K_x = 213 \pm 14 \times 10^3$ corresponding to a free energy of transfer of SecA from water to membrane of -7.1 ± 0.1 kcal mol^{-1} (Table 1). **(C)** Summary of fluorescence changes F/F_0 of each NBD label at 25 positions along the SecA sequence determined as in panels A and B. The data indicate strong interactions of SecA with the membrane at the N terminus, the NBD-II/HSD domains, and to a lesser extent the C-terminal domain (unstructured in crystallographic structures). **(D)** SecA structural domains: Nucleotide binding domain 1 (NBD-1, yellow), Preprotein crosslinking domain (PPXD, cyan), nucleotide binding domain-2 (NBD-2, green), Helix scaffold domain (HSD, grey), Helix wing domain (HWD, purple), and two-helix finger (2HF, blue).

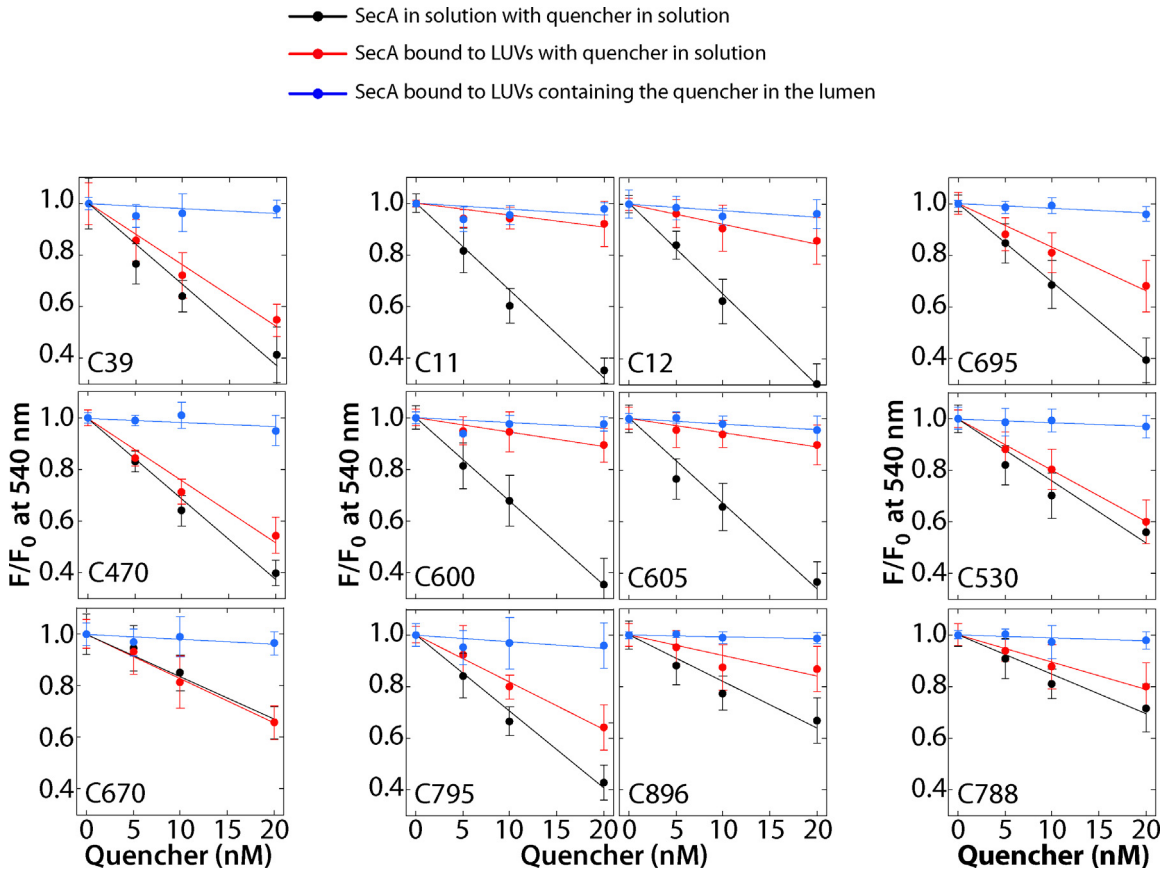

Figure 3. Labeled SecA residues do not penetrate across the membrane. If bound SecA were to penetrate across the membrane, then NBD-labeled residues that penetrate across should be accessible to fluorescent quenchers trapped within the vesicles. We tested this idea using the Uniblue (UB) quencher,[27] which was present either in solution (black line) in the absence of vesicles, outside the vesicles (red line) with bound SecA, or trapped within the vesicles (blue line). The ability of UB to quench NBD labels was determined for various cysteine residue positions based on our proposed membrane-associated topology. Left panel are residues exposed to the solvent, middle panel are residues embedded in the membrane, and right panel are residues close to the membrane (see Figure 2(C)). All fluorescence intensities were normalized to intensities at 540 nm.

(C, D)). This region contains an excess of 6 positively charged residues, all pointing toward the negatively charged membrane, constituting the second lipid binding domain in SecA (Figure 4(B)).

The C-tail region of SecA (cysteine mutants 795, 890 and 896) is a third, but relatively weak, lipid-binding domain previously described.[15] This structurally unstable region is missing from crystallographic and cryo-EM structures, but has been proposed to lie along the groove between the Pre-Protein Crosslinking Domain (PPDX) and NBD-II with its extremity close to the joint domain.[35] This is in good agreement with our observation. The C-tail of SecA (Residues 836–901) contains an excess of 5 positively charged residues.

All three lipid-binding domains carry an excess of positively charged residues that are conserved across species (Figure S3), consistent with the essential role of negatively charged lipid for SecA binding and function.[36] In contrast, the Helix Wing Domain (HWD) contains an excess of 9 negatively charged amino acids (Figure 4(A), right panel). This region of SecA must avoid tight association with the membrane because of electrostatic repulsion with negatively charged lipids. This hypothesis is supported by our NBD-fluorescence experiments (Figure 2(C)), because NBD probes at residues 695 and 721 reveal only a weak membrane interaction. These residues, conserved across species, suggests an important role of keeping the HWD away from the membrane.

Relative importance of the three lipid-binding domains

Wild-type SecA contains 7 tryptophan residues whose fluorescence changes upon membrane binding provide a convenient method of measuring the partitioning of SecA into membranes.[10] Briefly, we titrated various SecA mutants with large LUVs made from *E. coli* lipids and analyzed partitioning by the method of White *et al.*.[37] This approach

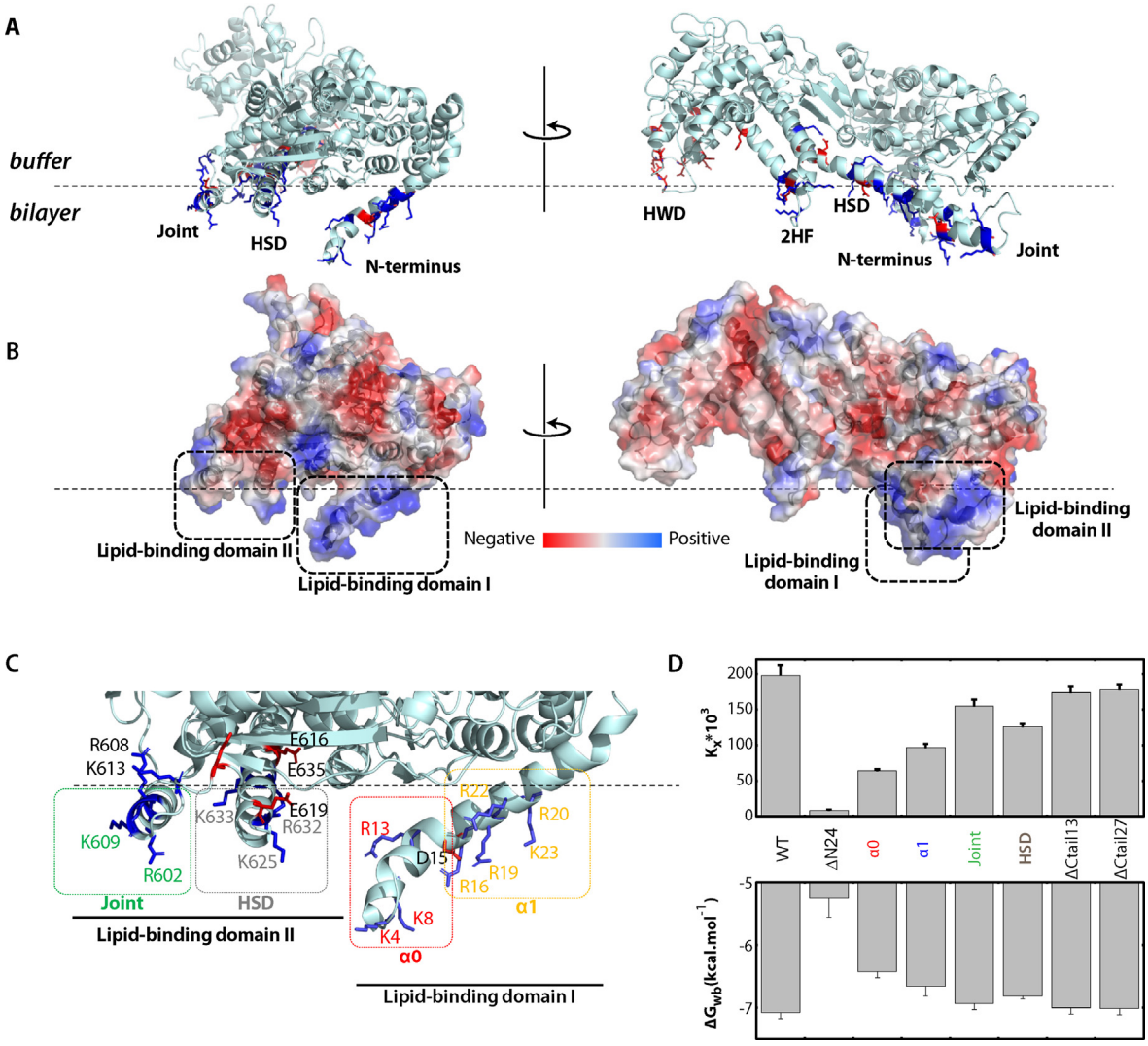

Figure 4. The distribution of surface charges of SecA are consistent with the topology determined by NBD labeling and fluorescence measurements. Positive charges dominate partitioning into the membrane. **(A)** *Ec*SecA crystal structure with the positively (blue) and negatively (red) charged residues facing the membrane interface highlighted as sticks. The Joint-Domain[35] that connects the helix scaffold domain (HSD) to the nucleotide binding domain II (NBD-II) are labeled. **(B)** The electrostatic potential-surface maps of *Escherichia coli* SecA displays areas of net positive charge highlighted in blue and areas of net negative charge highlighted in red. The map establishes two principal lipid binding domains labeled I and II. The charged residues at the membrane interface comprising Lipid-binding domains I and II can be subdivided as shown in order to examine the relative contributions of the four groups to binding strength. To investigate the relative strengths, four SecA mutants were designed whose positively charged residues were replaced with alanine: group α0 (K4A, K8A, and R13A; red) and group α1 (R16A, R19A, R20A, R22A, and K23A; blue) focused on the N-terminal helix-forming the lipid binding domain I. Lipid-binding domain II was subdivided into the joint domain (R602A and K609A; green) and the Helix Scaffold Domain (HSD, K625A, K632A, and K633A; grey). **(C)** The four SecA mutants (α0, α1, joint, and HSD) were titrated with LUVs made form *E. coli* lipids and the partition coefficients (K_x, top panel) and free energy of transfer from water to bilayer (ΔG_{wb}, bottom panel) were determined. **(D)** Summary of partition coefficients and free energies observed when the first 24 residues of the N terminus (ΔN24) are removed; or when the domains labeled in panel C were replaced with alanine residues; and finally, when the terminal C-tail is truncated by 13 or 27 residues (ΔCtail). Although all positively charged residues contribute to partitioning, the 27 residues of the N terminus clearly dominate partitioning.

allowed us to investigate the relative importance of the three identified lipid-binding domains (Figure 4). For reference the titration curve for WT-SecA with LUVs (Figure S4, black line) yields a partition coefficient (K_x) of 198,000, corresponding to a free energy of transfer from water-to-bilayer of -7.1 kcal mol^{-1} (Figure 4(C)), consistent with our previous measurements.

Table 1 Partitioning Free energies of SecA mutants.

Construct	[a]$K_x \times 10^{-3}$	[b]ΔG_{wb} (kcal mol^{-1})
WT	198 ± 11	−7.3
ΔN24	8.3 ± 12	−5.3
α0 (K4A + K8A + R13A)	64.4 ± 3	−6.4
R16A + R19A + R20A + R22A + K23A	97.0 ± 5	−6.7
R602A + K609A	155 ± 9	−6.9
K625A + R632A + K633A	126 ± 4	−6.8
ΔCtail13	174 ± 5	−7.0
ΔCtail27	178 ± 4	−7.0

[a] Mole-fraction partition coefficient.
[b] Free energy of transfer from water to bilayer.

Removing the first 24 residues of SecA (SecA ΔN24, Table 1) had a dramatic effect on SecA binding, as expected from previous observations,[5,14] demonstrating again the importance of the N terminus for SecA partitioning into the membrane. To investigate the role of the other positively charged domains, we designed two mutants based on the SecA crystal structures: SecA α0 where three positively charged amino acids (K4, K8, and R13) were mutated to alanine residues and SecA α1 where four residues (R16, R19, R20 and R22) were replaced by alanine (Figure 4(B)). In both cases, the alanine substitutions dramatically lowered the partitioning of SecA. The partition coefficient decreased by three-fold for SecA α0 and a two-fold for SecA α1 (Table 1).

The second lipid binding domain, located between the NBD-II and the HSD, consists of two α-helices (Figure 4(B)). We made two mutants lacking either the positively charged residues from the joint domain (K602A and K609A) or from the HSD (K625A, R632A, and K633A). Again, SecA partitioning was reduced in absence of these positive charges (Figure 4(C), Figure S4), causing the observed partition coefficient to be reduced by 25% for SecA-Joint and 35% for SecA-HSD, showing that this domain also plays a significant role in membrane binding (Table 1).

Finally, we used C-terminal truncated SecA mutants (1–888 and 1–874) lacking, respectively, 13 or 27 C-terminal residues of SecA that interact relatively weakly with the membrane[15] (Figure 2 (C)). As might be expected from the relatively weak binding of the third domain (residues 795, 890, and 896), the absence of the C-terminal residues did not result in a significant change in the binding to the membrane (Figure 4(C)), suggesting that the C-tail of SecA may be conformationally restricted from interacting strongly with the membrane.

Discussion

SecA is dimeric in solution but dissociates into monomers upon partitioning into LUV made with *E. coli* lipids.[11] This observation allowed us to examine the topology of monomeric SecA when bound to LUV. Starting from a collection of 25 mono-cysteine mutants of SecA, we covalently linked to each one separately the polarity-sensitive fluorophore NBD. From the changes in NBD-fluorescence upon vesicle binding, we determined the local polarity of each probe, and thereby the topology of the membrane-associated state of SecA (Figure 1, Figure 2(C)). The protein interacts with the membrane via three main lipid-binding domains that each carry an excess of surface-exposed positively charged residues that interact directly with the negatively charged LUV bilayer (Figure 4): (1) The amphipathic N terminus of the protein, known to penetrate the bilayer interface deeply,[14] (2) the Joint-Domain that connects to the Helix Scaffold Domain (HSD) to the Nucleotide Binding Domain II (NBD-II) whose amphipathic alpha-helical properties are similar to those of the N terminus region, and (3) the very flexible C-terminal tail of SecA, missing from x-ray and cryo-EM structures, but carrying an excess of 6 positively charged amino-acids that can potentially interact with the negatively charged headgroups of the lipids. We determined the relative importance of each lipid-binding domain by using mutants in which positively charged residues were replaced with alanine (Figure 4).

The N-terminal region is the most important lipid-binding domain; its interaction with the membrane is electrostatic in nature. This is supported by the fact that removal of some of positively charged residues resulted in weaker binding of the protein (Figures 4 (C) and S4). Positively charged residues located in the second lipid-binding domain comprised of the Joint Domain and the first half of the HSD also play a significant role in the binding of SecA to the membrane but are less important than those of the N-terminal helix. This second lipid-binding Domain likely helps stabilize the protein on the membrane, but it might also trigger a conformation change that results in better SecA affinity for the SecYEG complex as previously demonstrated.[5]

During protein translocation, SecA and SecYEG act as a functional unit. A crucial step in this process is the targeting of SecA to the cytoplasmic membrane. Although it has been known for a decade that anionic lipids are crucial for the SecA function,[9,38] the exact role of the mem-

brane has remained elusive. Over the last few years, a new step in SecA targeting to SecYEG has emerged. SecA was recently shown to gain access to the translocon via a lipid-bound intermediate state that induces a change in SecA conformation to prime it for high affinity binding to SecYEG[5] with membrane binding driven mainly by SecA's amphipathic N terminus.[14,17]

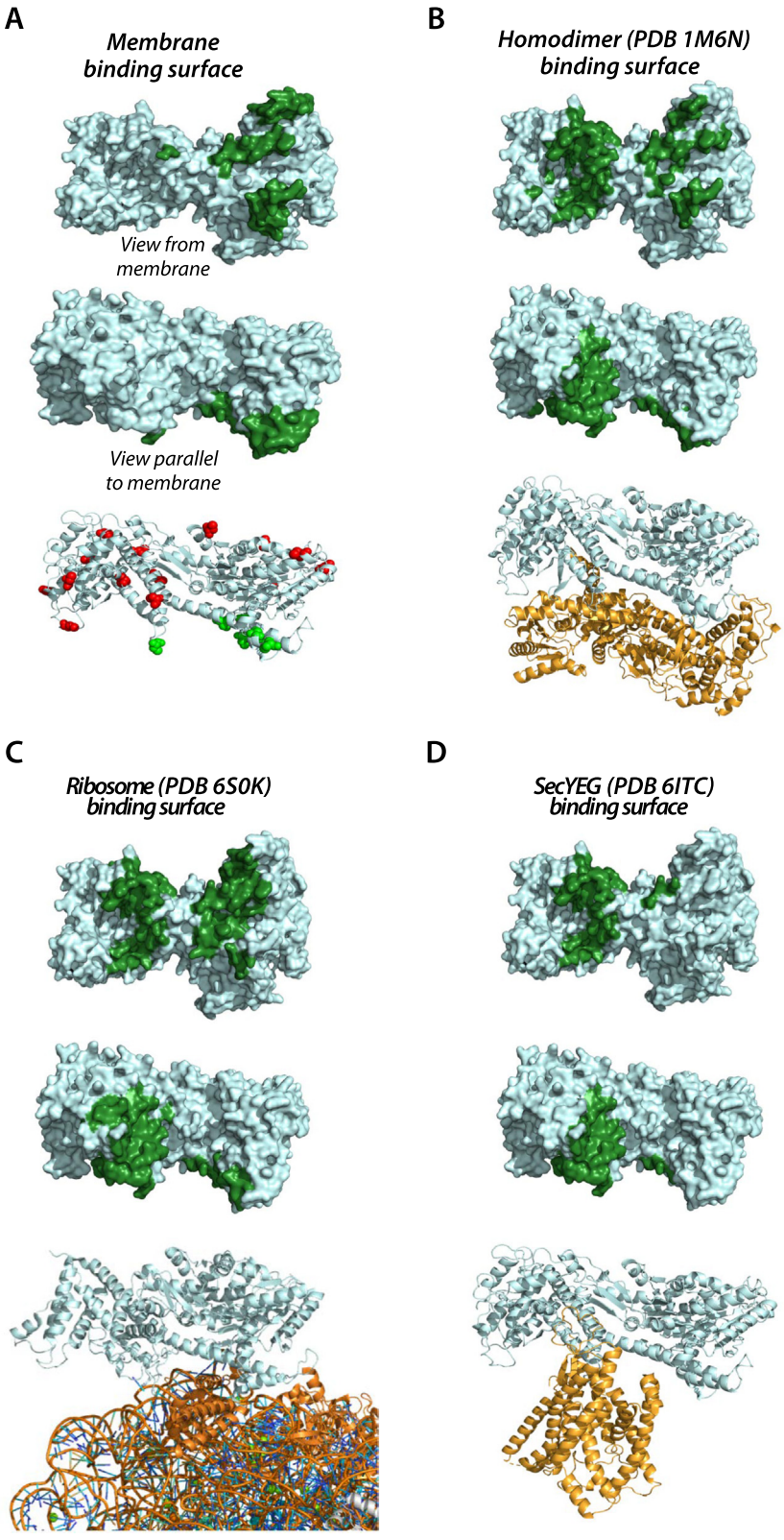

In our membrane-associated topology, the Helix Wing Domain (HWD) is close to the membrane. However, when NBD-probes were inserted in the HWD, no significant fluorescence intensity change was observed upon binding to LUVs (Figure 2(C), residues 696 and 721), meaning that this domain does not associate directly with the membrane under our conditions. This can be explained by the distribution of charged residues at the surface of the protein: the HWD domain carries an excess of negatively charged residues (Figure 4) that results in electrostatic repulsion from the negatively charged lipids. This enrichment is observed across different species (Figure S3), suggesting the importance of keeping the HWD off the membrane.

The membrane-facing surface that we have determined overlaps the interacting surface of SecA with other partners (Figure 5). A particularly interesting result is that the membrane binding surface of SecA is nearly identical to the surface involved in binding to the ribosome[39,40] (Figure 5 (C)). This implies two populations of SecA, consistent with the observation of Knüpffer et al. that membrane bound SecA is unable to bind to ribosomes.[41] The membrane-binding surface (Figure 5 (A)) is also similar to the homo-dimer interface observed in the cytoplasmic dimer[42–44] (Figure 5 (B)) and some of the SecA-SecY interaction surface recently observed by cryo-EM[45] (Figure 5(D), Figure S5). These interacting surfaces are located on the same side of SecA, suggesting an interplay between the different partners.

Our experimentally determined membrane-associated topology is very similar to the cryo-EM structure of SecA sitting on the translocon,[45] suggesting that the protein could easily move from the membrane to the SecY channel, while remaining attached to the membrane with both lipid-binding domains I and II and possibly the C-terminal tail, allowing it to hop on and off the translocon (see Figure S5) as proposed in the recent mechanistic model of Winkler et al.[17] In their model, the first step of SecA targeting to SecY involves an initial interaction of SecA with the membrane via its N terminus followed by a transition to a tighter bound state in which the protein partially inserts into the lipid bilayer with a lifetime of about ten of seconds in preparation for attachment to the membrane-embedded SecYEG channel.

Materials and Methods

Materials

All phospholipids were purchased form Avanti Polar Lipids (Alabaster, AL): *E. coli* total extract (catalog number 100500), 1-palmitoyl-2-oleoyl-glycero-3-phosphocholine (POPC, 850457), 1-palmytoyl-2-oleoyl-sn-glycero-3-phosphoethanolamine (POPE, 850757), 1-palmioyl-2-oleoyl-*sn*-glycero-3-phospho-(1′rac-glycerol) (POPG, 840457), and cardiolipin (841199). IANBD was purchased from Molecular Probes (Eugene, OR). Uniblue A vinyl sulfone was purchased from Sigma (St. Louis, MO).

Construction of mono-cysteine-mutants

Plasmids *pT7-C4-secA* encoding for *Escherichia coli* cysteine-less SecA and other mono-cysteine-mutants were a generous gift from Donald Oliver (see Table S1). Starting from the cysteine-less construction, single amino acid substitution was performed by PCR mutagenesis to introduce a single cysteine residue at different positions. Mutations were confirmed via DNA sequencing and complementation assays were used to confirm proper functioning of the mutants *in vivo* (Figure S1).

SecA Protein production

WT-SecA, mono-cysteine-SecA were obtained from *E. coli* BL21 (DE3) cells carrying the corresponding *secA* gene with a C-terminal His_6-tag under the control of the T5 promotor. Cells were grown in LB medium at 37 °C with constant shaking. Log-phase cultures (OD 0.8) were stimulated with IPTG (0.1 mM) for 2 hours at 30 °C. Cells were then harvested by centrifugation at 4,000 rpm for 15 minutes and the resulting pellet stored at −20 °C until needed.

Figure 5. One interface serves them all. On the ecSecA crystal structure (PDB 1M6N), we highlight in green the interaction surfaces of SecA under various conditions. **(A)** Residues interacting with the lipid bilayer represented in green, experimentally determined in this work. **(B)** Residues involved in the dimer interface of the cytoplasmic dimer. Residues in green are located within 6 Å of the second protomer (shown in orange in the bottom structure) of SecA (PDB: 1M6N).[48] **(C)** Amino-acids involved in the interaction with a ribosome synthetizing a nascent chain. Residues in green were determined to be within 6 Å of the RNC (PDB: 6S0K).[40] **(D)** SecA surface contacting the translocon with residues in green located within 6 Å of the SecY channel (PDB: 6ITC).[45] For the interaction with the membrane, the second protomer, the ribosomal complex, or the translocon, the residues of SecA involved in the contact are located on the same face of SecA. It is likely physiologically significant that the membrane binding surface (A) overlaps much of the ribosome binding surface (C).

SecA Protein purification

All protein purification steps and centrifugations were performed at 4 °C. Bacterial pellets (from 400 mL culture) were solubilized in 48 mL of Buffer A (50 mM Hepes-NaOH pH 7.4, 10 mM imidazole and 50 mM KCl) for 10 minutes at room temperature. Protease inhibitor cocktail (Roche) was added before the cell suspension was passed through a French Pressure Cell (SLM-Aminco) at 10,000 lb/in^2. The suspension was then centrifuged at 13,000*g* for 15 minutes to pellet the membrane fraction. The supernatant was loaded onto a Talon-Resin (1.5 × 5 cm) previously equilibrated with 25 mL of Buffer A. His-tagged SecA protein was then eluted with Buffer B (50 mM Hepes-NaOH pH 7.4, 200 mM imidazole, 50 mM KCl, 1 mM DTT). Two mL fractions were collected, and the protein profile analyzed using SDS-PAGE. Fractions containing 100 kDa SecA were then pooled, concentrated, and loaded onto a Superdex 200 increase 10/300 GL equilibrated in 50 mM Hepes-NaOH pH 7.4, 1 mM $MgCl_2$, and 50 mM KCl). SecA was then eluted at a flow rate of 0.5 mL/minute and protein elution monitored by optical absorbance at 280 nm. 500 μL fractions were collected and the protein profile analyzed using SDS-PAGE. Fractions containing the SecA protein were then pooled, and the protein concentration was estimated using the BioRad Assay with BSA as a reference and a molecular weight of 102 kDa.

NBD-Labeling of single-cysteine mutants of SecA

NBD-labeling was carried out in a 500 mM KCl solution to assure that SecA was monomeric.[18] The labeling was done using a standard procedure for the thiol-reactive derivative IANBD.[46] Briefly, SecA (2 mg) was first treated with 5 mM DTT for 20 minutes at 4 °C to reduce the cysteine residue. DTT was removed by passing the sample through a desalting PD-10 gel filtration column. In a typical labeling reaction, 5 μL of 0.4 M IANBD in DMSO was then mixed with 1 mL of a 2 mg/mL sample of single-cysteine SecA mutant in 25 mM Phosphate buffer pH 7.4 and 1 mM $MgCl_2$. The sample was incubated in the dark for two hours at room temperature or overnight at 4 °C. Samples were then passed through a second desalting PD-10 gel filtration column to remove excess IANBD.

Liposome preparation

Phospholipids dissolved in chloroform were dried under a stream of nitrogen and further dried under vacuum overnight. Lipids were then suspended in 25 mM Hepes-NaOH pH 7.4 and vortexed 15 minutes. Large unilamellar vesicles (LUVs) were prepared by extrusion. Lipid concentrations were determined according to the procedure of Bartlett.[47]

NBD-fluorescence

For topology experiments, NBD-labeled single-cysteine SecA (1 μM in 25 mM Phosphate Buffer pH 7.4, 50 mM NaCl, 100 mM KGlu, and 1 mM $MgCl_2$) was mixed with LUVs made from *E. coli* lipids (2 mM). To insure equilibration, we waited 30 minutes before measuring the fluorescence using an SLM 8000c spectrophotometer (Urbana, FL) equipped with double-grating excitation and single-grating emission monochromators. The measurements were made in 10 × 1 mm quartz cuvettes at 20 °C. Cross-orientation of polarizers were used to minimize scattering from the vesicles. Fluorescence spectra were obtained using an excitation wavelength of 470 nm. We averaged 10–15 scans collected over a 510–560 nm range using 1 nm steps. Excitation and emission slits were no wider than 8 nm. For the normalization of *F*/*F0*, we used a wavelength of 540 nm, which emission maximum of NBD in the absence of vesicles. The same conditions were used for recording scans in buffer alone, which were then subtracted from the appropriate peptide spectra. Three or more data sets were collected for all experiments.

NBD-fluorescence quenching by UniBlue dye

NBD-labeled single-cysteine SecA (1 μM in 25 mM Phosphate Buffer pH 7.4, 50 mM NaCl, 100 mM KGlu, and 1 mM $MgCl_2$) was mixed with LUVs made from *E. coli* lipids (4 mM), binding was allowed 30 minutes at 37 °C before measuring the fluorescence. UB (0.1% w/v) was then added directly in the aqueous phase and fluorescence was measured after 10 minutes incubation time.

Preparation of LUVs containing UB

Phospholipids dissolved in chloroform were dried under a stream of nitrogen and further dried under vacuum overnight. Lipids were then suspended in 25 mM Hepes-NaOH pH 7.4, and three different concentrations of UB dye (5, 10, and 20 nM) and vortexed 15 minutes. Large unilamellar vesicles (LUVs) were prepared by extrusion. The lipid vesicles were then passed twice through a PD10 desalting column to remove UB dye outside the vesicles. Lipid concentrations were determined according to the procedure of Bartlett.[47]

Tryptophan fluorescence

SecA (final dimeric concentration of 4 μM) was prepared in 50 mM Hepes-NaOH pH 7.4, 100 mM KGlu, 1 mM EDTA, 2 mM $MgCl_2$ and 1 mM DTT.

Fluorescence spectra were recorded at 37 °C with an SLM 8000c spectrophotometer (Urbana, FL) using an excitation wavelength of 295 nm and measuring the signal in the region of 310–400 nm (1 nm steps). Excitation and emission slits were not wider than 8 nm. Unless otherwise indicated, the emission polarizer was oriented at 0° relative to the vertical and the excitation polarizer at 90°. Spectra were measured using a 10 × 1 mm quartz cuvette. More than 10 spectra were averaged to achieve an adequate signal-to-noise ratio. The same conditions were used for recording scans in buffer alone, which were then subtracted from the appropriate peptide spectra. Three or more data sets were collected for all experiments.

DATA AVAILABILITY

Data will be made available on request.

Acknowledgements

This worked was supported by the National Institute of General Medical Sciences grant RO1 GM-74637 and R35 GM139652. We are pleased to acknowledge the outstanding technical support of Dr. Gargi Dasgupta. J.Z. is supported by NSF CCF 1763191, NIH R21 MD012867-01, NIH P30AG059307, NIH U01MH098953 and grants from the Silicon Valley Foundation and the Chan-Zuckerberg Initiative.

Author contributions

All authors conceived the experiments. Dr. Lindner was responsible for the molecular genetics. Dr. Roussel performed the fluorescence measurements. Drs. Roussel and White wrote the paper. All authors approved the final version of the manuscript.

Declaration of interests

The authors declare that they have no known competing financial interests or personal relationships that could have appeared to influence the work reported in this paper.

Appendix A. Supplementary material

Supplementary data to this article can be found online at https://doi.org/10.1016/j.jmb.2022.167607.

Received 16 March 2022;
Accepted 21 April 2022;
Available online 27 April 2022

Keywords:
partitioning free energy;
NBD-labeling;
fluorescence;
peripheral membrane protein;
membrane protein topology

1 Present address: Laboratory of Molecular Bacteriology, Department of Microbiology and Immunology, Rega Institute for Medical Research, KU Leuven, University of Leuven, Leuven, Belgium.

References

1. Gold, V.A.M., Whitehouse, S., Robson, A., Collinson, I., (2013). The dynamic action of SecA during the initiation of protein translocation. *Biochem. J.* **449**, 695–705.
2. Brundage, L., Hendrick, J.P., Schiebel, E., Driessen, A.J. M., Wickner, W., (1990). The purified *E. coli* integral membrane protein SecY/E is sufficient for reconstitution of SecA-dependent precursor protein translocation. *Cell* **62**, 649–657.
3. Lill, R., Cunningham, K., Brundage, L.A., Ito, K., Oliver, D., Wickner, W., (1989). SecA protein hydrolyzes ATP and is an essential component of the protein translocation ATPase of *Escherichia coli*. *EMBO J.* **8**, 961–966.
4. de Vrije, T., Batenburg, A.M., Jordi, W., de Kruijff, B., (1989). Inhibition of PhoE translocation across *Escherichia coli* inner-membrane vesicles by synthetic signal peptides suggests an important role of acidic phospholipids in protein translocation. *Eur. J. Biochem.* **180**, 385–392.
5. Koch, S., de Wit, J.G., Vos, L., Birkner, J.P., Gordiichuk, P., Herrmann, A., (2016). Lipids activate SecA for high affinity binding to the SecYEG complex. *J. Biol. Chem.* **291**, 22534–22543.
6. Cabelli, R.J., Dolan, K.M., Qian, L., Oliver, D.B., (1991). Characterization of membrane-associated and soluble states of SecA protein from wild-type and *SecA51(TS)* mutant strains of *Escherichia coli*. *J. Biol. Chem.* **266**, 24420–24427.
7. Chen, X., Xu, H., Tai, P.C., (1996). A significant fraction of functional SecA is permanently embedded in the membrane. *J. Biol. Chem.* **271**, 29698–29706.
8. Ulbrandt, N.D., London, E., Oliver, D.B., (1992). Deep penetration of a portion of *Escherichia coli* SecA protein into model membranes is promoted by anionic phospholipids and by partial unfolding. *J. Biol. Chem.* **267**, 15184–15192.
9. Ahn, T., Kim, J.-S., Lee, B.-C., Yun, C.-H., (2001). Effects of lipids on the interaction of SecA with model membranes. *Arch. Biochem. Biophys.* **395**, 14–20.
10. Roussel, G., White, S.H., (2020). Binding of SecA ATPase monomers and dimers to lipid vesicles. *Biochim. Biophys. Acta, Mol. Cell. Biol. Lipids* **1862**, 183112.
11. Roussel, G., White, S.H., (2020). The SecA ATPase motor protein binds to *Escherichia coli* lipid membranes only as monomers. *BBA – Biomembranes.* **1862**, 183358.
12. Breukink, E., Keller, R.C., de Kruijff, B., (1993). Nucleotide and negatively charged lipid-dependent vesicle aggregation caused by SecA. Evidence that SecA contains two lipid-binding sites. *FEBS Letters* **331**, 19–24.
13. Bauer, B.W., Shemesh, T., Chen, Y., Rapoport, T.A., (2014). A “push and slide” mechanism allows sequence-

insentive translocation of secretory proteins by the SecA ATPase. *Cell* **157**, 1416–1429.
14. Findik, B.T., Smith, V.F., Randall, L.L., (2018). Penetration into membrane of amino-terminal region of SecA when associated with SecYEG in active complexes. *Protein Sci.* **27**, 681–691.
15. Breukink, E., Nouwen, N., van Raalte, A., Mizushima, S., Tommassen, J., de Kruijff, B., (1995). The C terminus of SecA is involved in both lipid binding and SecB binding. *J. Biol. Chem.* **270**, 7902–7907.
16. Keller, R.C.A., (2011). The prediction of novel multiple lipid-binding regions in protein translocation motor proteins: A possible general feature. *Cell. Mol. Biol. Letters* **16**, 40–54.
17. Winkler, K., Karner, A., Horner, A., Hannesschlaeger, C., Knyazev, D., Siligan, C., (2020). Interaction of the motor protein SecA and the bacterial protein translocation channel SecYEG in the absence of ATP. *Nanoscale Adv.* **2**, 3431–3443.
18. Roussel, G., Lindner, E., White, S.H., (2019). Stabilization of SecA ATPase by the Primary cytoplasmic salt of *Escherichia coli*. *Protein Sci.* **28**, 984–989.
19. Chattopadhyay, A., (1992). Membrane penetration depth analysis using fluorescence quenching: A critical review. In: Gaber, B.P., Easwaran, K.R.K. (Eds.), *Biomembrane structure and function-The state of the art*. Adenine Press, pp. 153–163.
20. Wimley, W.C., White, S.H., (2000). Determining the membrane topology of peptides by fluorescence quenching. *Biochemistry* **39**, 161–170.
21. Fery-Forgues, S., Fayet, J.-P., Lopez, A., (1993). Drastic changes in the fluorescence properties of NBD probes with the polarity of the medium: Involvement of a TICT state? *J. Photochem. Photobiol., A* **70**, 229–243.
22. Wohland, T., Friedrich, K., Hovius, R., Vogel, H., (1999). Study of ligand–receptor interactions by fluorescence correlation spectroscopy with different fluorophores: Evidence that the homopentameric 5-hydroxytryptamine type 3_{As} receptor binds only one ligand. *Biochemistry* **38**, 8671–8681.
23. Ladokhin, A.S., Isas, J.M., Haigler, H.T., White, S.H., (2001). Interface-directed membrane insertion of proteins: From a general concept to an insertion pathway. *Biophys. J.* **80**, 539a-a.
24. Ladokhin, A.S., Isas, J.M., Haigler, H.T., White, S.H., (2002). Determining the membrane topology of proteins: Orientation of a D-E helix of annexin XII in the intermediate and inserted state. *Biophys. J.* **82**, 561a-a.
25. Crowley, K.S., Reinhart, G.D., Johnson, A.E., (1993). The signal sequence moves through a ribosomal tunnel into a noncytoplasmic aqueous environment at the ER membrane early in translocation. *Cell* **73**, 1101–1115.
26. Liao, S., Lin, J., Do, H., Johnson, A.E., (1997). Both lumenal and cytosolic gating of the aqueous ER translocon pore are regulated from inside the ribosome during membrane protein integration. *Cell* **90**, 31–41.
27. Ladokhin, A.S., Isas, J.M., Haigler, H.T., White, S.H., (2002). Determining the membrane topology of proteins: Insertion pathway of a transmembrane helix of annexin 12. *Biochemistry* **41**, 13617–13626.
28. Shatursky, O., Heuck, A.P., Shepard, L.A., Rossjohn, J., Parker, M.W., Johnson, A.E., (1999). The mechanism of membrane insertion for a cholesterol-dependent cytolysin: A novel paradigm for pore-forming toxins. *Cell* **99**, 293–299.
29. Raghuraman, H., Chattopadhyay, A., (2007). Orientation and dynamics of melittin in membranes of varying composition utilizing NBD fluorescence. *Biophys. J.* **92**, 1271–1283.
30. Jilaveanu, L.B., Oliver, D., (2006). SecA dimer cross-linked at its subunit interface is functional for protein translocation. *J. Bacteriol.* **188**, 335–338.
31. Ahn, T., Kim, H., (1994). SecA of *Escherichia coli* traverses lipid bilayer of phospholipid vesicles. *Biochem. Biophys. Res. Commun.* **203**, 326–330.
32. Schmidt, M.G., Rollo, E.E., Grodberg, J., Oliver, D.B., (1988). Nucleotide sequence of the *secA* gene and *secA* (Ts) mutations preventing export in *Escherichia coli*. *J. Bacteriol.* **170**, 3404–3414.
33. Wiener, M.C., White, S.H., (1992). Structure of a fluid dioleoylphosphatidylcholine bilayer determined by joint refinement of x-ray and neutron diffraction data. III. Complete structure. *Biophys J.* **61**, 434–447.
34. Papanikolau, Y., Papadovasilaki, M., Ravelli, R.B.G., McCarthy, A.A., Cusack, S., Economou, A., (2007). Structure of dimeric SecA, the *Escherichia coli* preprotein translocase motor. *J. Mol. Biol.* **366**, 1545–1557.
35. Gelis, I., Bonvin, A.M.J.J., Keramisanou, D., Koukaki, M., Gouridis, G., Karamanou, S., (2007). Structural basis for signal-sequence recognition by the translocase motor SecA as determined by NMR. *Cell* **131**, 756–769.
36. Breukink, E., Demel, R.A., de Korte-Kool, G., de Kruijff, B., (1992). SecA insertion into phospholipids is stimulated by negatively charged lipids and inhibited by ATP: a monolayer study. *Biochemistry* **31**, 1119–1124.
37. White, S.H., Wimley, W.C., Ladokhin, A.S., Hristova, K., (1998). Protein folding in membranes: Determining energetics of peptide-bilayer interactions. *Methods Enzymol.* **295**, 62–87.
38. Hendrick, J.P., Wickner, W., (1991). SecA protein needs both acidic phospholipids and SecY/E protein for functional high-affinity binding to the *Escherichia coli* plasma membrane. *J. Biol. Chem.* **266**, 24596–24600.
39. Singh, R., Kraft, C., Jaiswal, R., Sejwal, K., Kasaragod, V. B., Kuper, J., (2014). Cryo-electron microscopic structure of SecA bound to the 70S ribosome. *J. Biol. Chem.* **289**, 7190–7199.
40. Wang, S., Jomaa, A., Jaskolowski, M., Yang, C.-I., Ban, N., Shan, S., (2019). Molecular mechanism of cotranslational membrane protein recognition and targeting by SecA. *Nature Struct. Mol. Biol.* **26**, 919–929.
41. Knüpffer, L., Fehrenbach, C., Denks, K., Erichsen, V., Petriman, N.-A., Koch, H.-G., (2019). Molecular mimicry of SecA and signal recognition particle binding to the bacterial ribosome. *Am. Soc. Microbiol.* **10**
42. Wowor, A.J., Yan, Y., Auclair, S.M., Yu, D., Zhang, J., May, E.R., (2014). Analysis of SecA dimerization in solution. *Biochemistry* **53**, 3248–3260.
43. Chen, Y., Pan, X., Tang, Y., Quan, S., Tai, P.C., Sui, S.-F., (2008). Full-length *Escherichia coli* SecA dimerizes in a closed conformation in solution as determined by cryo-electron microscopy. *J. Biol. Chem.* **283**, 28783–28787.
44. Auclair, S.M., Oliver, D.B., Mukerji, I., (2013). Defining the solution state dimer structure of *Escherichia coli* SecA using Förster resonance energy transfer. *Biochemistry* **52**, 2388–2401.
45. Ma, C., Wu, X., Sun, D., Park, E., Catipovic, M.A., Rapoport, T.A., (2019). Structure of the substrate-engaged SecA-SecY protein translocation machine. *Nature Commun.* **10**, 2872.

46. Haugland, R.P., (1996). Handbook of Fluorescent Probes and Research Chemicals. Molecular Probes, Inc., Eugene, OR.
47. Bartlett, G.R., (1959). Phosphorus assay in column chromatography. *J. Biol. Chem.* **234**, 466–468.
48. Hunt, J.F., Weinkauf, S., Henry, L., Fak, J.J., McNicholas, P., Oliver, D.B., (2002). Nucleotide control of interdomain interactions in the conformational reaction cycle of SecA. *Science* **297**, 2018–2026.